Food Chemistry: X 20 (2023) 100964

Contents lists available at ScienceDirect

Food Chemistry: X

journal homepage: www.sciencedirect.com/journal/food-chemistry-x

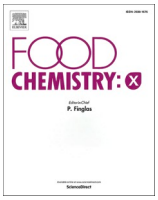

Exploring the formation of a transparent fat portion in bacon after heating based on physicochemical characteristics and microstructure

Han Wu [a], Zhifei He [a,b], Li Yang [a], Hongjun Li [a,b,*]

[a] College of Food Science, Southwest University, Chongqing 400715, China
[b] Chongqing Key Laboratory of Speciality Food Co-Built by Sichuan and Chongqing, Chongqing 400715, China

ARTICLE INFO

Keywords:
Physicochemical characteristics
Microstructure
Transparency
Fat portion
Bacon

ABSTRACT

Bacons, which possess a transparent fat tissue after heating, have high commercial value in China owing to their good sensory quality. This study was performed to explore the formation of transparent fat tissue by comparing the physicochemical characteristics and microstructures of transparent and non-transparent fat tissues. The physicochemical characteristics and microstructure of fat tissue were found to be significantly affected by drying, which increased the saturated fatty acid content and oxidation level, and decreased the moisture content and water activity ($p < 0.05$). Shrivelled adipocytes were observed in fat tissue after drying. Transparent and non-transparent fat tissues differed significantly in terms of moisture, fat content, texture, and fatty acid composition ($p < 0.05$). Multivariate statistical analysis indicated that low moisture content might be the major factor in the formation of transparent tissue, while the destruction of adipocytes also contributed to such formation.

1. Introduction

Traditional Chinese bacon is a popular dry-cured meat product made from pork belly cured with salt and dried via exposure to the sun or air-drying (smoking) (Guo et al., 2016; Yang et al., 2017). Due to its unique sensory characteristics and beneficial nutritional content, traditional Chinese bacon has gained popularity all over the world (Zhang et al., 2023; Li and Zhang, 2023). Typically, traditional Chinese bacon takes 1–2 months to produce, starting in November and ending in December of the Chinese lunar calendar. Southern China is suitable for bacon production due to its climate, with winter temperatures averaging 0–10℃ (Huang et al., 2014). Owing to its high salt concentration, bacon does not require refrigeration during transportation and storage, and can be conveniently consumed via steaming, boiling, or frying (Xie et al., 2008).

The color of meat products is widely considered the most important factor influencing the purchasing desires of consumers (Xu et al., 2019). Previous research on bacon coloration has mainly focused on lean portions (Walsh et al., 1998). Although minimal research has been performed on the presence of the fat portion in bacon, this portion plays a vital role in the consumer selection process (McLean et al., 2017). Prior study investigating fat quality measures to characterize the suitability of pork bellies for commercial bacon production found that white, firm fat is better than soft, oily, wet, gray, or floppy fat (Seman et al., 2013). In traditional Chinese bacon produced in Anhui province, called *dao-ban-xiang*, the fat portion has a light amber color, dense tissue, and good elasticity (Wang et al., 2022). In general, studies on the quality of bacon fat have focused on the suitability of the material or consumer preference; changes in bacon fat after processing have not been investigated.

Interestingly, the fat portion of the bacon becomes transparent after boiling. This phenomenon has a significantly positive effect on the sensory attributes of the product. Bacon with transparent fat is considered a high-quality product with better commercial value (Zhu et al., 2023; Gan et al., 2019; Huang et al., 2022; Wang et al., 2022). However, only few studies have investigated the mechanisms by which fat becomes transparent after heating.

Based on preliminary research, translucency is postulated to be related to the extent of fat (Maw et al., 2003). A higher percentage of linoleic and α-linolenic acids (unsaturated fatty acids) has a positive impact on translucency, whereas increased levels of myristic, palmitic and stearic acids (saturated fatty acids) have a negative effect. This fact could be attributed to the lower melting points of unsaturated fatty acids than associated saturated fatty acids; fat tissue with a higher proportion of unsaturated fatty acids was less solid and more translucent at the

* Corresponding author at: College of Food Science, Chongqing Engineering 13 Research Center of Regional Food, Southwest University, No.2 Tiansheng Road, Beibei 14 District, Chongqing 400715, China.
E-mail address: swujournal@163.com (H. Li).

https://doi.org/10.1016/j.fochx.2023.100964
Received 1 March 2023; Received in revised form 7 October 2023; Accepted 23 October 2023
Available online 7 November 2023

same temperature. Although the main fatty acids in bacon are monounsaturated fatty acids, particularly oleic acid, the fatty acid composition of different pig breeds causes significant differences in the final product (Huang et al., 2014; Latin et al., 2022; Okon et al., 2021; Wu et al., 2022). However, the occurrence of transparent fat tissue may not have an association with any particular breed, suggesting a deeper explanation for transparency. Other studies have revealed that fat tissue transparency is associated with temperature (Sasaki et al., 2006). The melting curves of porcine adipose tissues were investigated using differential scanning calorimetry, and the appearance of porcine adipose tissues became clear during heating, which was attributed to the phase transition occurring between the onset temperature and the conclusion temperature 1. The transparency of the samples was also more pronounced at conclusion temperature 2 than at conclusion temperature 1. Accordingly, the researchers considered that another, similar phase transition occurred between conclusion temperatures of 1 and 2. Although heating for melting is necessary, not all fat tissues become transparent after heating. Further investigation is required to clarify this phenomenon.

Determining whether adipose tissue is transparent requires an evaluation criterion. However, the transparency of the adipose tissue is difficult to measure. No indicator or equipment can be used to directly and accurately reflect the transparency of fat tissue as it is not similar to glass, film, or solution, which are homogeneous systems. Adipose tissue is a loose connective tissue formed by tightly packed adipocytes enclosed within an extracellular matrix that provides a scaffold for adipocytes and is composed of proteins, proteoglycans, and polysaccharides (Javier Ruiz-Ojeda et al., 2019). The propagation of light in adipose tissue is affected by several factors that induce absorbance or refraction. A spectrophotometer is poorly suited for obtaining the correct transmittance owing to the unreliable light intensity of the material. Existing studies measured fat transparency by inserting a pin parallel to the fat surface and assessing the visibility of the pin (Maw et al., 2003). This method depends on the perception of researchers, and requires professional assessors with extensive training. In another study, the transparency of the squid mantle was analyzed using the coefficient of transmission of inverter luminescence (Kugino et al., 2009). An image of the sample recorded by a digital camera was converted into a 1064 × 712 pixel 16-bit grayscale image. The transparency of the samples was then analyzed based on the blackness of the images. This method is not suitable for assessing the opacity of bacon fat tissue as the materials are highly dissimilar in size, texture, and homogeneity, and the necessary professional-grade devices and software are not readily available. Therefore, a combination of sensory and instrumental methods to determine the transparency of the fat portion may provide more objective results. In this study, sensory evaluation and the transmittance of the fat portion in the visible wavelength range were used to comprehensively evaluate the transparency of the fat portion. Simple and reliable methods for measuring transparency provide dependable data for investigating the formation of transparent fat tissue.

Consumers prefer bacon that has a transparent fat tissue (TFT) after boiling owing to its attractive appearance; thus, such bacon has a higher commercial value. From an economic perspective, commercial bacon producers should understand the influencing factors that result in fat tissue becoming transparent. However, this topic has not been addressed in the literature. Not only Chinese bacon, but this study can also provide valid information to improve the quality of the fat portion of typical dry-cured meat products in the world, such as ham, sausage, and shoulder. This study aimed to explore these factors by comparing the physicochemical properties and microstructures of transparent and non-transparent bacon fat tissues.

2. Materials and methods

2.1. Samples

Three samples—of two different types of processed bacon and a portion of fresh pork belly—were purchased from Yonghui Supermarket (Beibei, Chongqing).

The first sample comprised bacon with TFT, and had been commercially processed as follows: the 'green bacon' was dry-cured for 3 days in a 4 % salt (m/m) mixture at 4℃, drained for one day at 4℃, dried via hot air (approximately 50℃) for 2 days, and then air-dried for 1 month at room temperature.

The second bacon sample had non-transparent fat tissue (NFT). The curing process was similar, except for hot-air drying and the air-drying time was reduced to 3–7 days.

For comparison, fresh pork belly was processed into bacon in the laboratory to obtain the fat tissue. The pork belly was cut into 20 × 5 × 4 cm pieces (length × width × thickness), dry-cured, and drained according to the process described for the purchased bacon. At this point, samples were collected from both the outer layer (BDO) and inner layer fat tissues (BDI). The pork belly was then dried via hot air for 2 days at 55℃. The obtained fat tissue had two different appearances: the outer layer (approximately 3–4 mm) was transparent whereas the inner layer was non-transparent. After drying, samples of both the outer layer (ADO) and inner layer (ADI) fat tissue were collected.

2.2. Evaluation of transparency

The transparency of the bacon fat tissue was measured via sensory evaluation and transmissivity. The transparency of the fat tissue was scored via sensory evaluation using the following categories: 1 = non-transparent, 2 = slightly transparent, 3 = translucent, 4 = turbidly transparent, and 5 = transparent. Ten trained penellists (five males and five females, with average age of 26 years) participated in the sensory evaluation. The optical transmittance of the fat tissue (cut into slices of 2–3 mm) was measured using a spectrometer (F-2000, Hitachi, Tokyo, Japan) in the wavelength range of 390—–780 nm. The spectrum was collected; the transmittance is expressed as the average value in the wavelength range of 390–780 nm.

2.3. Moisture and fat content and water activity (Aw)

The moisture and fat content of each sample were measured according to a previously described method (Tan et al., 2021). Briefly, the moisture contents were determined by drying the fat tissue samples in an oven at 105℃ until constant weight was achieved. Thereafter, the samples were cooled and reweighed. The fat content of each sample was determined using Soxhlet extraction. The Aw was measured at 25℃ using a water activity meter (Huake, Wuxi, China).

2.4. Lipid extraction

Lipids were extracted according to a described method with some modifications (Folch et al., 1957). The samples (15.0 g) were minced and mixed with 150 mL of a chloroform/methanol solution (2:1, v/v) and left to stand for 24 h at 4℃. The mixture was equilibrated twice with 20 mL sodium chloride solution (0.9 %, w/w), and the solvent phase was filtered using qualitative filter paper and anhydrous sodium sulphate. Finally, the extract was evaporated using a rotary evaporator (N1300DW, Xinnuokai, Beijing, China) at 40℃ to harvest the total lipids.

2.5. Lipid oxidation analysis

The peroxide value (POV) was determined according to a described method, with some modifications (Fan et al., 2022). Total lipids (2–3 g)

were mixed with 30 mL of a chloroform glacial acetic acid solution (2:3, v/v) and 1 mL saturated potassium iodide solution, shaken until the lipids dissolved completely, and left to stand for 3 min in the dark. Thereafter, 100 mL of water was added and titrated with sodium thiosulfate standard solution (0.01 M) until the solution turned light yellow. Finally, 1 mL of starch indicator was added and titrated until the blue faded; the results are expressed as milliequivalent peroxide/kg lipid.

Thiobarbituric acid reactive substance (TBARS) values were measured according to a previously described method, with some modifications (Li et al., 2019). Briefly, the sample (2 g) was minced and homogenized in 30 mL of 7.5 % trichloroacetic acid (TCA). Thereafter, 5 mL of the mixture was filtered and incubated with 5 mL of 0.02 M thiobarbituric acid (TBA) solution for 40 min in a water bath at 100℃. After cooling to room temperature, the absorbance of the solution was measured at 532 nm using a microplate reader (Biotek, Santa Clara, CA, USA). The TBARS values were calculated based on a standard malondialdehyde (MDA) curve; the results are expressed as mg MDA/kg lipid. Each determination was performed in triplicate.

The acid value (AV) was determined using a described method (Guo et al., 2019). Total lipid (20 g) was dissolved in 100 mL of an isopropanol ether (1:1, v/v) solution and titrated with 0.1 M potassium hydroxide solution to the phenolphthalein endpoint. The solvent was titrated as a blank for calibration; the results are expressed as milligrams of potassium hydroxide consumed per gram of oil.

2.6. Fatty acid composition analysis

Fatty acid composition was determined using a previously described method with some modifications (Xu et al., 2022). First, the lipids were converted into fatty acid methyl esters (FAMEs). The total lipids (0.1 g) were mixed with 8 mL of 0.5 M methanolic sodium hydroxide solution and incubated at 80℃ until the lipid droplets were completely dissolved. Thereafter, 7 mL of a boron trifluoride-methanol ($\omega = 14$ %) solution was added as a derivatizing agent, and the sample was kept in a water bath for 5 min. After cooling to room temperature, hexane (3 mL) and saturated NaCl solution (10 mL) were added, and the sample was shaken for 10 s and left to stand for 1 h. The upper phase was filtered via a 0.22 μm filtration membrane and collected in a sample vial. The FAMEs were measured using a Shimadzu GC-2010 Plus chromatograph (Shimadzu, Kyoto, Japan) equipped with an AOC-20i auto-injector and a flame ionization detector (FID). The separation was carried out using a DB-FastFAME column (30 m × 0.25 mm, 0.25 μm, Agilent, Santa Clara, USA). The oven temperature was kept at 80℃ for 1 min, raised to 165℃ at a rate of 40℃/min, held at 165℃ for 1 min, increased to 230℃ at a rate of 4℃/min, and held for 4 min. Nitrogen was used as a carrier gas at a constant pressure of 12 psi. The temperatures of the injection port and the FID were 250℃ and 260℃, respectively. Fatty acids were identified by comparing their retention times with those of commercial methyl ester standards (37-component FAME mix; Anpel, Shanghai, China). The results are expressed as the percentage of each fatty acid.

2.7. Texture profile analysis

Texture profile analysis (TPA) was performed according to a previously delineated method with some modifications (Xu et al., 2022). Puncture tests were performed using a TA-XT Plus texture analyzer (Stable Micro Systems, Surrey, England) equipped with a cylindrical stainless-steel probe (P/50, 50 mm diameter). The samples were cut into pieces with dimensions of 2 cm × 2 cm × 1 cm (length × width × height). All tests were performed at a speed of 2 mm/s to a depth of 5 mm using a 2-cycle sequence. The interval between the two compressions was 5.0 s and the trigger force was set to 5 g. The hardness, springiness, cohesiveness, chewiness, and resilience were also measured. The test was implemented at 40 ± 2℃ and 8 samples were measured for each condition.

2.8. Thermal analysis using differential scanning calorimetry (DSC)

DSC was performed according to a described method using a DSC 4000 calorimeter (PerkinElmer, Waltham, MA, USA) (Paszkiewicz et al., 2020). The samples (10 mg) were weighed, placed in aluminium pans, and fixed onto the sample platform. An empty aluminium pan was used as the baseline reference. The samples were subjected to the following temperature program: cooled to –40℃, held for 10 min, and heated to 80℃ at a rate of 5℃/min. The peak temperatures at maximum heat absorption T (℃) were collected in triplicate.

2.9. Histological analysis

The samples were prepared for observation by light microscopy (LM) according to a previously described method with some modifications (Field et al., 2021). Briefly, the samples were cut to a size of 5 mm × 5 mm × 1 mm (length × width × height) and placed in 4 % paraformaldehyde at 4℃ overnight. The tissues were dehydrated in increasing concentrations of ethanol, embedded in paraffin, sectioned into 4–8 μm slices using a microtome (HM 340E, Thermo Scientific, Waltham, USA), and stained with haematoxylin and eosin. The samples were observed using a digital microscopy scanner with Pannoramic MIDI (3DHISTECH, Budapest, Hungary).

A scanning electron microscope (SEM) (SU3500, Hitachi High Technologies Corporation, Tokyo, Japan) was used to visualize the microstructure, according to a described method (Zhuang et al., 2016). The samples were cut into cubes (5 mm × 5 mm × 3 mm) and fixed with 0.1 M phosphate buffer (pH 7.0) containing 2.5 % (w/v) glutaraldehyde for 24 h at 4℃. The fixed tissues were post-fixed in 1 % (w/v) osmium tetroxide solution for 20 h. The postfixed tissues were washed in triplicate with 0.1 M phosphate buffer (pH 7.0) for 20 min and then dehydrated in an ethanol series. Finally, the tissues were dried and sputter-coated with gold for visualizing.

2.10. Statistical analysis

All data were analyzed using SPSS (version 24.0; SPSS Inc., Chicago, USA) with Duncan's method. The results are expressed as the mean value ± standard error. Orthogonal projections to latent structures discriminant analysis (OPLS-DA) were used for multivariate analysis using SIMCA 14.1 software (Umetrics, Sweden). The variable importance in projection (VIP) values in the OPLS-DA model were calculated to identify the contributions of different factors. was All tests were performed in triplicate unless otherwise specified. Significant difference was indicated by $p < 0.05$.

3. Result and discussion

3.1. Comparison of the transparency of different adipose tissues

The transparency of fat tissue is not controllable because the mechanism of formation of transparent tissue is not clear. Therefore, two types of commercial bacon with transparent and non-transparent fat tissue were used to compare with laboratory-prepared bacon, which the outer layer of the fat portion appeared transparent and the inner layer showed non-transparent. The transparency of the various samples, as evaluated via the senses and spectrophotometer, is presented in Fig. 1 and Table 1. Fig. 1 clearly shows the differences in transparency among the different fat tissues. The TFT had the best transparency among the samples. Light spots in the illuminated background were observed, similar to those in the black background (except for a part at the edge because the tissue did not cling to the background). Meanwhile, neither the illuminated background nor the black background could be observed through the NFT, indicating that it had the worst transparency. By comparing ADO and ADI (see Fig. 1; the red and blue arrows point to ADO and ADI, respectively), light spots and the black background can

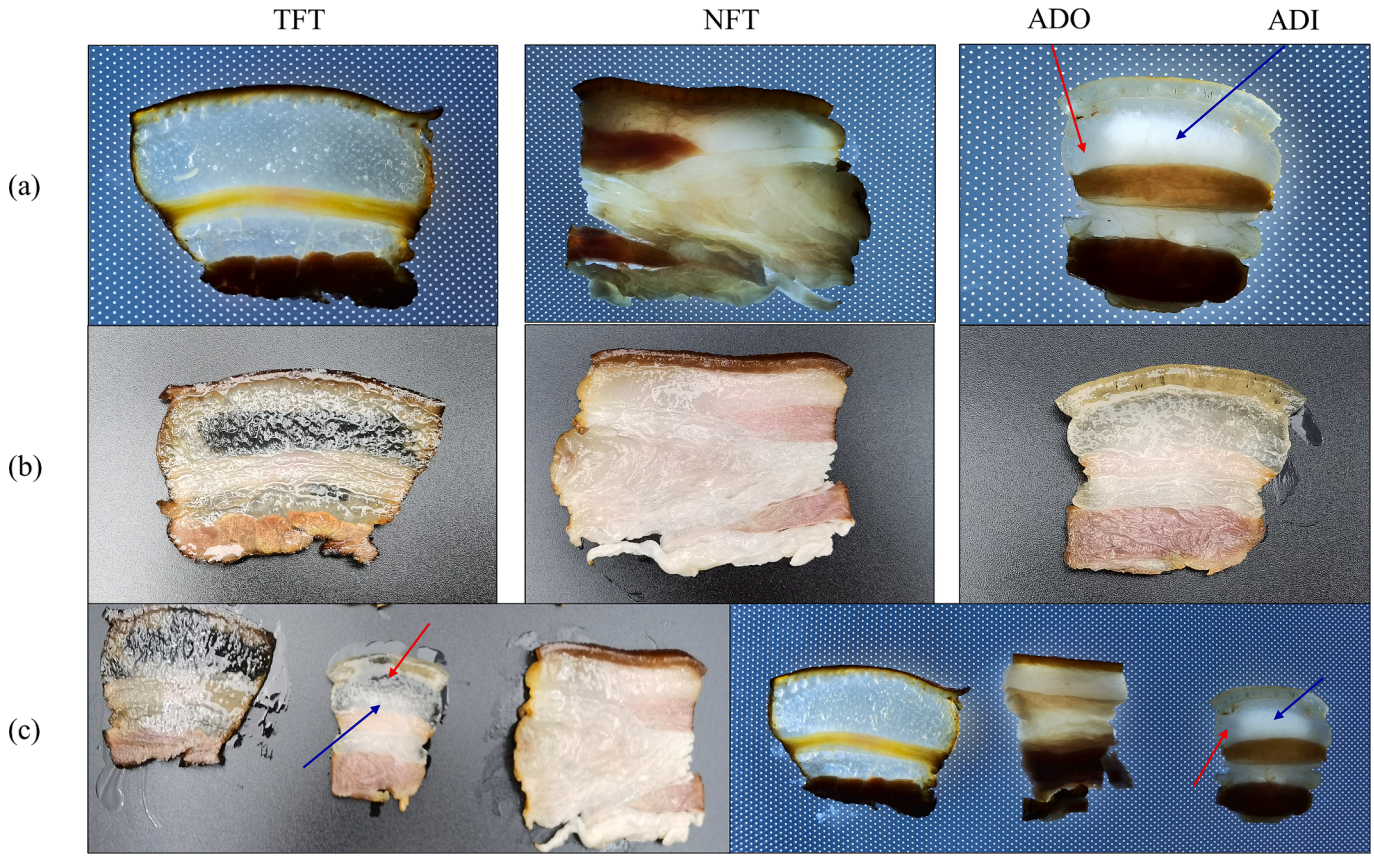

Fig. 1. The appearance of different bacon fat tissues photographed in illuminated and black backgrounds. Note: Row (a) is the fat tissue photographed on an illuminated background; Row (b) is shot on black ground. Simultaneous images of different fat tissues against the two backgrounds are shown in row (c). The red arrow pointed to the ADO and the blue arrow pointed to the ADI. (For interpretation of the references to color in this figure legend, the reader is referred to the web version of this article.)

Table 1
Transparency analysis via different methods.

Measurements	TFT	NFT	BDI	BDO	ADI	ADO
Sensory evaluation	4.75 ± 0.46^{c}	1.38 ± 0.52^{a}	1.13 ± 0.35^{a}	1.25 ± 0.46^{a}	1.38 ± 0.74^{a}	4.00 ± 0.53^{b}
Transmittance (%)	29.83 ± 3.80^{c}	0.48 ± 0.13^{a}	0.45 ± 0.11^{a}	0.57 ± 0.10^{a}	0.59 ± 0.11^{a}	18.88 ± 1.93^{b}

Note: Values with different letters in the same raw are significantly different ($p < 0.05$).

only be observed vaguely through ADO, marking its transparency as worse than that of TFT. In contrast, the transparency of ADI was similar to that of NFT. The sensory evaluation results shown in Table 1 are consistent with those shown in Fig. 1. It can be seen that the BDI and BDO are not displayed in Fig. 1, because they are not the fat portion from finished products have the lowest transparency. The panel considered the TFT to be the most transparent, and rated the transparency of the ADO as acceptable, despite its slight turbidity. Other tissues were classified as non-transparent fat tissues.

The spectra and transmittance results for different adipose tissues in the visible light region (390–780 nm) are shown in Fig. 2 and Table 1. The curves indicate that TFT and ADO had relatively high visible light transmittance (between 24.54 % and 36.65 % and 14.72 % to 23.67 %, respectively), whereas the other four types of adipose tissues allowed almost no visible light passage (less than 1 %). Under photopic vision, yellow-green light with a middle wavelength of 555 nm is the brightest to the human eye (Chen et al., 2019). The transmittance of the TFT and

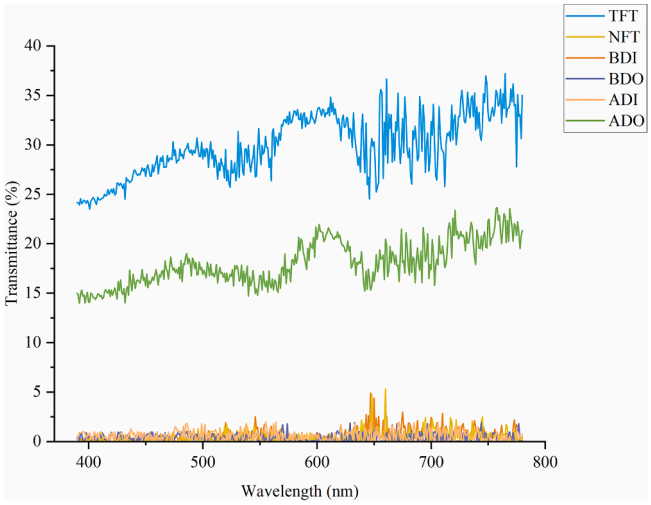

Fig. 2. The transmittance spectra of different bacon fat tissue for the wavelength range of 380–780 nm.

ADO at 555 nm was significantly higher, whereas that of the TFT (29.37 %) was 12.59 % higher than that of the ADO (16.78 %) ($p < 0.05$). The average transmittance of the TFT was 29.83 %, which was significantly higher than that of the ADO (18.88 %), whereas those of the other samples were less than 1 % ($p < 0.05$). However, compared with the findings of the sensory evaluation method, the transmittance value was relatively low for ADO. This finding may be attributed to the yellow

color of the ADO sample, which affects the transmittance to a certain degree. However, color did not have a strong influence on transparency in the sensory evaluation; therefore, ADO still had acceptable transparency.

3.2. Comparison of the physicochemical characteristics of different adipose tissue

The physicochemical characteristics of subcutaneous bacon fat are shown in Table 2. Moisture and fat are the two principal components of bacon fat tissue, accounting for 10–20 % and 70–80 %, respectively (Hugo et al., 2022). In this study, the moisture and fat contents of the bacon fat tissue ranged from 3 % to 9 % and 89 % to 95 %, respectively. This difference might be attributed to the fresh pork used in the former studies, while the sample used in this study was dried. However, the moisture and fat contents in bacon fat tissue are similar to those in pork after stewing (Xu et al., 2022). Collagen contracts after heating, inducing the shrinkage of fibers and increasing cooking losses (Purslow, 2018). Therefore, the lower moisture content was not only due to air drying but also collagen contraction. During drying, the membranes of adipocytes were destroyed, and the melted triglycerides leaked out, resulting in fat oozing from the surface of the bacon adipose tissue. However, the fat content increased with a decrease in the moisture content. This result is mainly attributable to the faster transfer of water than fat, which increases the relative fat content (Li et al., 2016; Xu et al., 2022). Of note, transparent fat tissue has a significantly lower moisture content (3.10–4.18 %) than non-transparent fat tissue (6.52–9.02 %) ($p < 0.05$). The Aw of bacon fat tissue was between 0.531 and 0.714, which is similar to the results of an earlier study (Zhang et al., 2021). A strong correlation was found between Aw and moisture content. The Aw was lower in transparent fat tissue (0.531–0.596) than in non-transparent fat tissue (0.621–0.714). The moisture content and Aw in the outer fat tissue layer (7.30 % and 0.633 before drying, 4.18 % and 0.596 after drying) were significantly lower than those in the inner fat tissue layer (9.02 % and 0.714 before drying, 7.01 % and 0.621 after drying, respectively), both before and after drying ($p < 0.05$). Water in the fat tissue evaporated during drying; the process occurred faster in the outer fat tissue layer than in the inner layer, resulting in the outer fat tissue layer losing significant moisture content and Aw during drying ($p < 0.05$).

Lipid oxidation is one of the main parameters of meat products. The oxidation level was determined by the presence of primary or secondary products of lipid oxidation. The POV can determine the early stages of oxidation by measuring the amount of hydroperoxides, whereas the TBARS value reflects the amount of secondary oxidation products (Abeyrathne et al., 2021). The TBARS value and POV of the bacon fat tissue samples ranged from 0.56 to 1.66 mg MDA/kg and 0.62–2.89 meq peroxide/kg lipid, respectively. This result is similar to that of prior research that aimed to determine the oxidation level during smoking (Huang et al., 2014). In this study, the TBARS value and POV of transparent fat tissue were not significantly different from those of non-transparent fat tissue ($p > 0.05$). Although TFT had the longest air-drying time, the highest value was observed for NFT. POV can decrease owing to the decomposition of hydroperoxides, resulting in the formation of carbonyls or other breakdown products. The TBARS values revealed a trend similar to that of POV in bacon fat tissue. The TBARS value decrease as the aldehydes degraded or further reacted with themselves or other compounds, such as amino acids and Maillard reaction intermediates (Huang et al., 2014). Therefore, the POV and TBARS values of the TFT were lower than those of the NFT owing to the longer air-drying time. Before drying, the oxidation level of the fat tissue did not differ significantly between the inner and outer layers ($p > 0.05$). However, the fat tissue after drying had a significantly higher oxidation level ($p < 0.05$), especially in the outer layer of the fat tissue, where contact with air and temperature were both relatively higher.

AV reflects free fatty acid content, which is a vital indicator for evaluating the degree of lipid hydrolysis (Gu et al., 2017). The TFT had the highest AV, which was attributed to the longest drying time, resulting in lipid hydrolysis into free fatty acids. Drying with hot air can increase the temperature of fat tissue, accelerating of lipid hydrolysis. Therefore, the AV of the fat tissue after drying was higher, especially in the outer layer ($p < 0.05$). However, no significant difference in AV was observed between transparent and non-transparent fat tissue ($p > 0.05$).

Table 2
Physicochemical characters of bacon subcutaneous fat from different samples.

Parameter	Adipose tissue					
	TFT	NFT	BDO	BDI	ADO	ADI
Moisture content (%)	3.1 ± 0.03^{a}	6.52 ± 0.08^{c}	7.3 ± 0.13^{d}	9.02 ± 0.28^{e}	4.18 ± 0.22^{b}	7.01 ± 0.15^{d}
Fat content (%)	94.75 ± 0.31^{e}	92.55 ± 0.34^{c}	91.93 ± 0.1^{b}	89.78 ± 0.43^{a}	93.14 ± 0.26^{d}	91.50 ± 0.18^{b}
Aw	0.53 ± 0.01^{a}	0.65 ± 0.01^{e}	0.63 ± 0.00^{d}	0.71 ± 0.00^{f}	0.60 ± 0.01^{b}	0.62 ± 0.01^{c}
TBARS (mg MDA/kg)	0.56 ± 0.10^{a}	1.66 ± 0.12^{e}	0.74 ± 0.05^{bc}	0.63 ± 0.03^{ab}	0.93 ± 0.03^{d}	0.83 ± 0.01 ^{cd}
AV (mg/g)	1.86 ± 0.02^{e}	1.69 ± 0.09^{d}	0.31 ± 0.01^{a}	0.42 ± 0.02^{b}	0.40 ± 0.02^{b}	0.49 ± 0.04^{c}
POV (milliequivalent peroxide/kg lipid)	1.69 ± 0.01^{c}	2.89 ± 0.08^{e}	0.62 ± 0.01^{a}	0.64 ± 0.03^{a}	1.86 ± 0.02^{d}	1.22 ± 0.02^{b}

Note: Values with different letters in the same raw are significantly different ($p < 0.05$).

3.3. Comparison of the melting properties of different adipose tissues

The complexity of the thermal behaviors of oils and fats can be attributed to the variety of triacylglycerols that they primarily contain. Therefore, the fats and oils did not exhibit specific melting or crystallization temperatures. DSC is widely used in the thermal analysis of fat or oil to provide information on the melting and crystallization behaviors. The melting point of fat tissue is influenced by its chemical structure, including fatty acid and triacylglycerol composition, whereas the thermal properties of triacylglycerol are affected by fatty acid composition and its distribution to triglycerides. Triacylglycerols can be further divided into four categories: triunsaturated, monosaturated-diunsaturated, desaturated-monounsaturated, and trisaturated (Embaby et al., 2022). The melting points of the four triacylglycerols increase sequentially. Fig. 3 illustrates the DSC curves of the bacon fat tissue during heating from –40℃ to 80℃. In the melting profile, three endothermal peaks (1, 2, and 3) were observed; the triacylglycerols were mainly melted at peaks 2 and 3. The peak temperatures of peak 1 ranged from –19.48℃ to –16.94℃, which might represent the melting of triunsaturated triacylglycerol due to its lower melting temperature. The monosaturated-diunsaturated and desaturated-monounsaturated triacylglycerol had a higher melting point; thus the peak temperature of peak 2 was observed between –0.89℃ and 2.18℃. Peak 3 might correspond to the phase transition of trisaturated triacylglycerol, which had the highest melting point; the peak temperatures were between 27.13℃ and 30.37℃ (Paszkiewicz et al., 2020). Unsaturated fatty acids are easily oxidized during drying at high temperatures. Therefore, the disappearance of peak 1 in the melting profiles of TFT and ADO, indicates that unsaturated fatty acids may be oxidized to saturated fatty acids or other secondary products. Additionally, the offset temperatures of peak 3 were between 30.52℃ and 34.33℃; thus, the bacon fat tissue melted as the temperature exceeded 34.33℃.

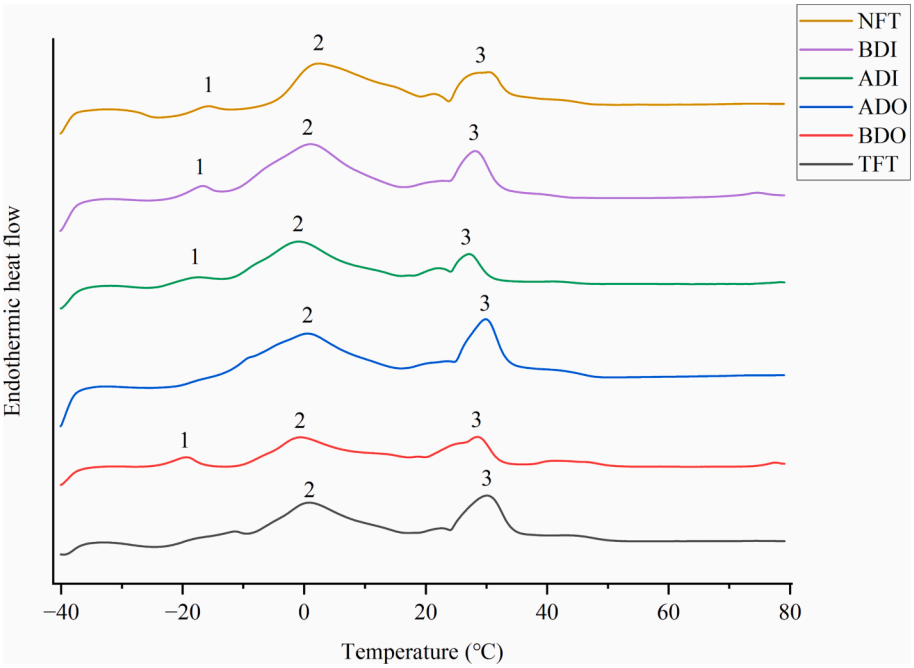

Fig. 3. Differential scanning calorimetry (DSC) curves indicating endothermic heat flow for different bacon fat tissues.

3.4. Comparison of fatty acid composition of different adipose tissues

The fatty acid composition of fat tissue is closely related to product quality, including its melting point, hardness, oxidation stability, nutrition, and flavor (Tu et al., 2021). In the present study, the fatty acid compositions of different fat tissues were compared to investigate their effects on transparency. As shown in Table 3, 24 fatty acids were detected, of which 11 were saturated and 13 were unsaturated. The fatty acid profiles were similar across the various fat tissues in the samples. MUFA (monounsaturated fatty acid) were the main fatty acids, particularly oleic acid, which accounted for 40.49–46.47 %. Palmitic acid (21.76–26.75 %) and linoleic acid (10.18–17.16 %) were the major components of SFA (saturated fatty acid) and PUFA (polyunsaturated fatty acid). This result is consistent with that of former studies that investigated the fatty acid composition of meat after cooking (Li et al., 2016; Xu et al., 2022). The SFA content in the fat tissue increased after drying, whereas the UFA content decreased significantly ($p < 0.05$). A similar comparison was observed between the outer and inner layers of fat tissue; the UFA content in the outer layer was significantly lower than that in the inner layer ($p < 0.05$). Hot air drying is a powerful promoter of lipid oxidation during bacon processing. Therefore, UFA was oxidized to SFA owing to its unsaturated molecular structure, which more easily induces a chain reaction of free radicals. Additionally, the SFA content in transparent fat tissue was significantly ($p < 0.05$) higher (41.16–43.08 %) than that in non-transparent fat tissue (34.59–39.24 %). Meanwhile, transparent fat tissue presented lower UFA content than non-transparent fat tissue. This conclusion seems to contradict previous results, where increased UFA content was found to have a positive impact on transparency (Maw et al., 2003). This result might be because earlier studies attributed the increased transparency to lower melting points, and a higher UFA content could decrease the melting point of fat tissue. However, regardless of whether the fat tissue was transparent, all temperatures used in this study exceeded the melting point. Therefore, the effects of melting point-related factors on the transparency can be ignored. The influence of fatty acid composition on transparency requires further investigation; however, transparency might be mainly attributable to the drying process, and the changes in fatty acid composition are only affected by drying.

3.5. Comparison of texture of different adipose tissues

The texture of the fat tissue has a significant influence on its sensory quality. Similar to other soft materials, fat tissue acts as an elastic solid that can withstand mechanical stress (Wijarnprecha, et al., 2022). The mechanical strength of adipose tissue is related to the density of adipocytes. While the protein network preferentially deforms in regions lacking adipocytes to absorb the strain, the cells primarily absorb the strain in locations with a lot of adipocytes. Different ways of absorbing strain could present in the TPA results. The TPA results for fat tissue in this study are presented in Table 4S. Hardness and chewiness are the most important indicators of the bacon fat tissue. Generally, the ratio of saturated to unsaturated fatty acids in fat tissue is highly correlated with hardness. The increased proportion of saturated fatty acids (such as C16:0 and C18:0) and the decrease in unsaturated fatty acids (such as C18:2n6) were found to correlate with higher hardness. The highest hardness occurred in ADO (10017.80 g) while the lowest occurred in BDI (2136.25 g). An increasing trend in hardness was observed in fat tissue after drying, particularly in the outer layer. These results differed from those of a previous study, indicating that the hardness of porcine subcutaneous fat decreased during long-term stewing. Connective tissue was solubilized during stewing; however, the bacon fat tissue could not be solubilized after drying. Studies on fat tissue texture are usually conducted in a coagulation state. However, the deformation behavior of fat tissue is closely related to the temperature, solidity, and coherence of the fat phase and extracellular matrix (Wijarnprecha, et al., 2022). Some researchers have investigated the mechanical behavior of fat tissue, indicating that texture is dependent on adipocyte-centric factors under physiological temperatures, such as cell size and shape, size distribution, volume fraction, spatial distribution, extent of cell–cell interactions, and phase continuity (Kruglikov, 2014). Once the temperature of fat tissue exceeded 37℃, the texture was dictated by the collagen network surrounding the adipocytes due to the melting state of fat in the adipocytes (Comley & Fleck, 2010; Wijarnprecha, Fuhrmann, et al., 2022). Therefore, the hardness of fat tissue in this study did not correlate with the composition of fatty acids because the fat in adipocytes was melted. The increased hardness and chewiness of the dried fat tissue could be attributed to moisture loss, destruction of adipocytes, and shrinkage and cross-linking of the connective tissue during drying. Springiness and

Table 3
Contents of fatty acids composition in different fat tissue.

FA (%)	TFT	NFT	BDO	BDI	ADO	ADI
C4:0	0.03 ± 0.00^{a}	0.04 ± 0.01^{a}	0.03 ± 0.00^{a}	0.04 ± 0.01^{a}	0.03 ± 0.00^{a}	0.03 ± 0.00^{a}
C8:0	0.05 ± 0.00^{c}	0.01 ± 0.00^{b}	0.01 ± 0.00^{a}	–	0.01 ± 0.00^{a}	0.01 ± 0.00^{a}
C10:0	0.05 ± 0.00^{ab}	0.06 ± 0.00^{bc}	0.06 ± 0.00^{abc}	0.06 ± 0.01^{c}	0.06 ± 0.00^{bc}	0.05 ± 0.00^{a}
C12:0	0.07 ± 0.00^{c}	0.06 ± 0.00^{b}	0.06 ± 0.00^{b}	0.06 ± 0.01^{b}	0.06 ± 0.00^{b}	0.05 ± 0.00^{a}
C14:0	1.31 ± 0.09^{c}	1.09 ± 0.02^{ab}	1.13 ± 0.01^{b}	1.15 ± 0.05^{b}	1.12 ± 0.00^{ab}	1.05 ± 0.00^{a}
C14:1	0.02 ± 0.00^{d}	–	0.01 ± 0.00^{a}	0.01 ± 0.00^{c}	0.01 ± 0.00^{b}	0.01 ± 0.00^{a}
C15:0	0.03 ± 0.00^{a}	0.04 ± 0.00^{e}	0.04 ± 0.00^{d}	0.04 ± 0.00^{de}	0.03 ± 0.00^{c}	0.03 ± 0.00^{b}
C16:0	26.75 ± 0.70^{c}	22.15 ± 0.21^{a}	23.08 ± 0.00^{b}	21.76 ± 0.20^{a}	22.85 ± 0.12^{b}	23.72 ± 0.00^{c}
C16:1	2.24 ± 0.08^{e}	1.32 ± 0.01^{a}	1.42 ± 0.05^{b}	2.14 ± 0.04^{d}	1.60 ± 0.03^{c}	1.38 ± 0.01^{ab}
C17:0	0.19 ± 0.03^{a}	0.24 ± 0.00^{b}	0.27 ± 0.01^{d}	0.24 ± 0.01^{b}	0.19 ± 0.00^{a}	0.18 ± 0.00^{a}
C17:1	0.22 ± 0.04^{bc}	0.20 ± 0.00^{b}	0.20 ± 0.00^{b}	0.24 ± 0.01^{c}	0.17 ± 0.00^{a}	0.15 ± 0.00^{a}
C18:0	14.25 ± 0.36^{d}	13.13 ± 0.09^{c}	12.09 ± 0.42^{b}	10.88 ± 0.27^{a}	16.47 ± 0.43^{e}	13.77 ± 0.09^{d}
C18:1	41.49 ± 0.09^{b}	40.49 ± 0.19^{a}	45.68 ± 0.21^{e}	46.47 ± 0.56^{f}	42.93 ± 0.30^{c}	43.73 ± 0.03^{d}
C18:2n6t	0.10 ± 0.01^{b}	0.07 ± 0.00^{a}	0.06 ± 0.00^{a}	0.10 ± 0.01^{b}	0.07 ± 0.00^{a}	0.06 ± 0.00^{a}
C18:2n6c	10.18 ± 0.88^{a}	17.16 ± 0.17^{e}	12.53 ± 0.22^{c}	13.63 ± 0.14^{d}	11.27 ± 0.19^{b}	12.67 ± 0.05^{c}
C18:3n6	–	–	0.02 ± 0.00^{b}	–	–	0.01 ± 0.00^{a}
C18:3n3	0.66 ± 0.22^{a}	1.07 ± 0.00^{c}	0.88 ± 0.02^{b}	0.85 ± 0.06^{b}	0.57 ± 0.01^{a}	0.53 ± 0.00^{a}
C20:0	0.27 ± 0.02^{a}	0.36 ± 0.09^{b}	0.29 ± 0.00^{ab}	0.27 ± 0.01^{a}	0.31 ± 0.01^{ab}	0.31 ± 0.00^{ab}
C20:1	1.05 ± 0.18^{b}	1.02 ± 0.00^{a}	1.01 ± 0.04^{a}	0.89 ± 0.04^{a}	1.02 ± 0.02^{a}	1.06 ± 0.01^{b}
C20:2	0.59 ± 0.06^{a}	0.89 ± 0.01^{d}	0.66 ± 0.00^{b}	0.68 ± 0.03^{b}	0.78 ± 0.01^{c}	0.76 ± 0.01^{c}
C20:3n6	0.08 ± 0.01^{a}	0.11 ± 0.00^{d}	0.08 ± 0.00^{ab}	0.09 ± 0.00^{c}	0.09 ± 0.00^{bc}	0.08 ± 0.00^{abc}
C20:4n6	0.17 ± 0.03^{a}	0.24 ± 0.00^{c}	0.16 ± 0.00^{a}	0.21 ± 0.01^{b}	0.22 ± 0.00^{b}	0.21 ± 0.00^{b}
C20:3n3	0.12 ± 0.01^{b}	0.18 ± 0.01^{d}	0.15 ± 0.01^{c}	0.15 ± 0.01^{c}	0.10 ± 0.00^{a}	0.10 ± 0.00^{a}
C24:0	0.07 ± 0.02^{b}	0.10 ± 0.00^{c}	0.09 ± 0.01^{c}	0.09 ± 0.00^{bc}	0.05 ± 0.00^{a}	0.05 ± 0.00^{a}
SFA	43.08 ± 0.90^{d}	37.27 ± 0.03^{b}	37.15 ± 0.42^{b}	34.59 ± 0.56^{a}	41.16 ± 0.57^{d}	39.24 ± 0.09^{c}
UFA	56.92 ± 0.90^{a}	62.73 ± 0.03^{c}	62.85 ± 0.42^{c}	65.45 ± 0.56^{d}	58.84 ± 0.57^{b}	60.76 ± 0.09^{b}
MUFA	45.02 ± 0.30^{b}	43.02 ± 0.19^{a}	48.32 ± 0.23^{e}	49.75 ± 0.49^{f}	45.74 ± 0.36^{c}	46.33 ± 0.03^{d}
PUFA	11.90 ± 1.11^{a}	19.72 ± 0.16^{e}	14.53 ± 0.19^{c}	15.70 ± 0.08^{d}	13.10 ± 0.21^{b}	14.43 ± 0.07^{c}

Note: SFA, monounsaturated fatty acid; UFA, unsaturated fatty acid; MUFA, monounsaturated fatty acid; PUFA, polyunsaturated fatty acid. For each component, data with different superscript letters differ significantly at $p < 0.05$. "–", Not detected.

cohesiveness did not differ between transparent and non-transparent fat tissue; however, both had an insignificantly higher level before drying owing to intact fat cells and the extracellular matrix.

3.6. Comparison of microstructure of different adipose tissues

Fat tissue is composed of adipocytes surrounded by an extracellular matrix. The extracellular matrix mainly consists of two collagen-based structures: the basement membrane and interlobular septa. The collagen I fiber network builds interlobular septa, providing a frame for the formation of an open-cell 3D foam. The basement membrane consists of a collagen IV mesh that behaves as a closed-cell foam. Adipocytes are embedded in an extensive collagenous extracellular matrix that is penetrated by a network of blood vessels (Alkhouli et al., 2013). The diameter of a typical adipocyte ranges from 50 to 200 μm. No specific investigations have been performed on the microstructure of bacon fat tissue; therefore, no reference was available to compare the changes in microstructure.

Fig. 4S shows the microstructure of bacon fat tissue. The adipocytes appeared polydisperse and were roughly spheroidal cells with a diameter of approximately 100 μm. The extracellular matrix was clearly visible via SEM and is indicated by black arrows in Fig. 4S (a). The structure of adipocytes can remain intact prior to drying in hot air. However, with the destruction of cell membranes and shrinkage of collagen during drying, triacylglycerol is melted and squeezed out from the adipocytes (Xu et al., 2022). Lard dripping was observed during drying. In Fig. 4S (a), the adipocytes in TFT appeared shriveled and cell 'sockets' are exposed (red arrows in TFT) (Wijarnprecha, et al., 2022). A flat adipocyte can be observed in Fig. 4S (a) (red arrows in ADO), which may not have completely lost its triacylglycerol content. However, adipocytes in ADI maintained their complete structures. This result might be because the temperature inside the bacon was not high enough or the triacylglycerol could not easily leak out from the adipocytes during drying. The observed bacon fat tissue microstructure was not similar to the microstructure of the subcutaneous back fat after stewing; the difference in the processing methods meant that collagen gelation was not observed in bacon fat tissue (Xu et al., 2022).

LM was used to examine the microstructure of the bacon fat tissue, and the results are shown in Fig. 4S (b). As the outer fat tissue layers (BDO and ADO) were closer to the skin, more abundant connective tissue and blood vessels were observed. Due to the different observation methods, LM could not present the 3D structure of adipocytes. As a result, the difference between fat tissues appeared less dramatic because it was difficult to observe the shriveled adipocytes directly. Voids caused by the loss of triacylglycerol were filled again during paraffin embedding; however, some subtle differences were still observed. Before drying, the boundary of adipocytes in the fat tissue was smooth and round, whereas the cell boundary of the fat tissue after drying displayed an atrophic and depressed shape, as circled in Fig. 4S (b). Thus, significant differences between the microstructures of transparent and non-transparent fat tissue could be observed; these differences might contribute to changes in physicochemical properties. The loss of lipids and destruction of adipocytes could be factors in the transformation of fat tissue to a transparent state.

3.7. Multivariate analysis via OPLS-DA

OPLS-DA can explain the variation between and within groups using distinct predictions and orthogonal components. This method can eliminate independent variables that have little correlation with classification, and screen out the characteristic variables of the samples. As a supervised recognition method, OPLS-DA can effectively classify samples and establish discriminant models (Kang et al., 2022). As shown in Fig. 5S, the two groups of transparent and non-transparent fat tissue were successfully discriminated using OPLS-DA. The transparent fat tissue (round points) was distributed in the second and third quadrants, whereas the non-transparent fat tissue (triangular points) was located in the first and fourth quadrants. The OPLS-DA model provided a good explanation of the variance and prediction ability ($R^2X = 0.671$, $R^2Y = 0.989$, $Q^2 = 0.978$). The model was not overfitted according to the permutation test findings from this analysis, which revealed R^2 and Q^2 Y-axis intercept values of 0.395 and –0.854, respectively, after 200 permutations. To clarify the differences between the transparent and non-transparent fat tissue, the physicochemical characteristics with VIP values exceeding 1.0 were defined as potential volatile marker compounds, and were considered to play a crucial role in the OPLS-DA discrimination process. As shown in Fig. 5S, 18 physicochemical

characteristics were filtered, including hardness, moisture content, chewiness, SFA and UFA content, Aw, fat content, and several types of fatty acids. Correlation analysis was conducted using these indicators, and the results are shown in Fig. 6S. Transmittance and sensory evaluation were positively correlated with fat content, hardness, chewiness, SFA, C8:0, C16:0, and C14:1. Moisture content, Aw, springiness, UFA, C15:0, C20:3n3, C17:0, and PUFA negatively correlated with transmittance and sensory evaluation. However, this correlation is not necessarily the direct cause of transparent fat tissue formation. Of note, texture was also correlated with moisture content and Aw. The fat content and Aw were correlated with the moisture content. In summary, the change in texture was attributed to the moisture content and strictions of adipocytes and connective tissue; however, these factors could not be the reason for the formation of transparent tissue. The fatty acid composition might be affected by oxidation during drying. Other physicochemical characteristics, such as Aw and fat content, were closely correlated with moisture content; therefore, the low moisture content of fat tissue had a high probability of resulting in the formation of transparent fat tissue.

The present study is exploratory; therefore, the exact mechanism by which the moisture-induced formation of transparent tissue occurs remains unclear. Adipose tissue containing abundant moisture is speculated to resemble water-in-oil emulsions. As the moisture concentration decreased, the transparency of the 'emulsions' increased gradually. The existing state of water in the adipose tissue and the influence of drying require further investigation.

4. Conclusion

The aim of this study was to explore the formation mechanism of transparent fat tissue of bacon. Physicochemical properties and microstructures of transparent and non-transparent fat tissue were compared, and multivariate statistical analysis was performed to screen the key factors. Drying significantly affected the physicochemical characteristics and microstructure of bacon fat. The SFA content, hardness, and oxidation level increased after drying, whereas the moisture, UFA content, and Aw decreased. Destruction of adipocytes was also observed in transparent fat tissue. However, not all physicochemical characteristics differed significantly between transparent and non-transparent tissue. The results of OPLS-DA revealed that the formation of transparent fat tissue was most probably influenced by the low moisture content. However, the mechanism underlying the effect of water on adipose tissue transparency requires further research. Transparency of fat tissue with gradient moisture can be investigated in the future to refine the mechanism of transparent fat formation. This study provides a theoretical basis for the production of bacon comprising transparent fat.

CRediT authorship contribution statement

Han Wu: Conceptualization, Methodology, Formal analysis, Investigation, Writing – original draft. **Zhifei He:** Supervision. **Li Yang:** Visualization. **Hongjun Li:** Funding acquisition.

Declaration of Competing Interest

The authors declare that they have no known competing financial interests or personal relationships that could have appeared to influence the work reported in this paper.

Data availability

Data will be made available on request.

Acknowledgments

This work supported by Chongqing Technology Innovation and Application Development Special Key Project (Grant No. CSTB2022TIAD-KPX0380); Collaborative innovation and key technology of rabbit industry in Sichuan and Chongqing (Grant No. 2022YFQ0033); China Agriculture Research System of MOF and MARA (Grant No. CARS-43-E-2).

Appendix A. Supplementary data

Supplementary data to this article can be found online at https://doi.org/10.1016/j.fochx.2023.100964.

References

Abeyrathne, E., Nam, K., & Ahn, D. U. (2021). Analytical methods for lipid oxidation and antioxidant capacity in food systems. *Antioxidants, 10*(10), 1587. https://doi.org/10.3390/antiox10101587

Alkhouli, N., Mansfield, J., Green, E., Bell, J., Knight, B., Liversedge, N., … Winlove, C. P. (2013). The mechanical properties of human adipose tissues and their relationships to the structure and composition of the extracellular matrix. *American Journal of Physiology-Endocrinology and Metabolism, 305*(12), E1427–E1435. https://doi.org/10.1152/ajpendo.00111.2013

Chen, Y., Ho, H., Lai, Y., Nagao, T., & Hsueh, C. (2019). Thermochromic vanadium dioxide film on textured silica substrate for smart window with enhanced visible transmittance and tunable infrared radiation. *Infrared Physics and Technology, 102*, Article 103019. https://doi.org/10.1016/j.infrared.2019.103019

Comley, K., & Fleck, N. A. (2010). The toughness of adipose tissue: Measurements and physical basis. *Journal of Biomechanics, 43*(9), 1823–1826. https://doi.org/10.1016/j.jbiomech.2010.02.029

Embaby, H. E., Miyakawa, T., Hachimura, S., Muramatsu, T., Nara, M., & Tanokura, M. (2022). Crystallization and melting properties studied by DSC and FTIR spectroscopy of goldenberry (Physalis peruviana) oil. *Food Chemistry, 366*, Article 130645. https://doi.org/10.1016/j.foodchem.2021.130645

Fan, L., Xian, C., Tang, S., Ding, W., Xu, C. H., & Wang, X. C. (2022). Effect of frozen storage temperature on lipid stability of hepatopancreas of Eriocheir sinensis. *LWT-Food Science and Technology, 154*, Article 112513. https://doi.org/10.1016/j.lwt.2021.112513

Field, S. L., Marrero, M. G., Liu, L., Penagaricano, F., & Laporta, J. (2021). Histological and transcriptomic analysis of adipose and muscle of dairy calves supplemented with 5-hydroxytryptophan. *Scientific Reports, 11*(1), 9665. https://doi.org/10.1038/s41598-021-88443-w

Folch, J., Lees, M., & Stanley, G. H. (1957). A simple method for the isolation and purification of total lipides from animal tissues. *Journal of Biological Chemistry, 226*(1), 497–509.

Gan, X., Li, H., Wang, Z., Emara, A. M., Zhang, D., & He, Z. (2019). Does protein oxidation affect proteolysis in low sodium Chinese traditional bacon processing? *Meat Science, 150*, 14–22. https://doi.org/10.1016/j.meatsci.2018.10.007

Gu, X., Sun, Y., Tu, K., & Pan, L. (2017). Evaluation of lipid oxidation of Chinese-style sausage during processing and storage based on electronic nose. *Meat Science, 133*, 1–9. https://doi.org/10.1016/j.meatsci.2017.05.017

Guo, X., Huang, F., Zhang, H., Zhang, C., Hu, H., & Chen, W. (2016). Classification of traditional Chinese pork bacon based on physicochemical properties and chemometric techniques. *Meat Science, 117*, 182–186. https://doi.org/10.1016/j.meatsci.2016.02.008

Guo, Y., Liang, X., Bi, J., Ling, R., Jiang, Y., Mou, Z., … Qin, W. (2019). A polyamidoamine-mediated competitive colorimetric assay based on gold nanoparticles for determining acid values in edible sunflower seed, corn and extra virgin olive oils. *Food Chemistry, 285*, 450–457. https://doi.org/10.1016/j.foodchem.2019.01.177

Huang, Y., Li, H., Huang, T., Li, F., & Sun, J. (2014). Lipolysis and lipid oxidation during processing of Chinese traditional smoke-cured bacon. *Food Chemistry, 149*, 31–39. https://doi.org/10.1016/j.foodchem.2013.10.081

Huang, X., Luo, J., Lou, A., Zhou, B., Luo, S., & Shen, Q. (2022). Effect of liquid smoking temperature on the lipid properties of Chinese bacon. *Food Research and Development, 43*(11), 157–163. in chinese.

Hugo, A., Wyngaard, B. E., Strydom, P. E., Witt, F. H., Pohl, C. H., & Kanengoni, A. T. (2022). The effect of dietary Echium oil supplementation on the fatty acid profile, omega-3 fatty acid content and subcutaneous fat quality of pork. *Livestock Science, 257*, Article 104833. https://doi.org/10.1016/j.livsci.2022.104833

Javier Ruiz-Ojeda, F., Mendez-Gutierrez, A., Maria Aguilera, C., & Plaza-Diaz, J. (2019). Extracellular Matrix Remodeling of Adipose Tissue in Obesity and Metabolic Diseases. *International Journal of Molecular Sciences, 20*(19), 4987. https://doi.org/10.3390/ijms20194888

Kang, C., Zhang, Y., Zhang, M., Qi, J., Zhao, W., Gu, J., … Li, Y. (2022). Screening of specific quantitative peptides of beef by LC-MS/MS coupled with OPLS-DA. *Food Chemistry, 387*, Article 132932. https://doi.org/10.1016/j.foodchem.2022.132932

Kruglikov, I. L. (2014). General theory of body contouring: 2. Modulation of mechanical properties of subcutaneous fat tissue. *Journal of Cosmetics, Dermatological Sciences and Applications, 2014*(4), 117–127. https://doi.org/10.4236/jcdsa.2014.42017

Kugino, M., Kugino, K., Tamura, T., & Asakura, T. (2009). Relationship between tissue structural collapse and disappearance of flesh transparency during postmortem changes in squid mantles. *Journal of Food Science, 74*(9), E495–E501. https://doi.org/10.1111/j.1750-3841.2009.01351.x

Latin, K., Mastanjevic, K., Raguz, N., Bulaic, M., Luzaic, R., Heffer, M., & Lukic, B. (2022). Differences in fatty acid profile and physical-chemical composition of slavonska slanina-dry cured smoked bacon produced from black slavonian pig and modern pigs. *Animals, 12*(7), 924. https://doi.org/10.3390/ani12070924

Li, B., Xu, Y., Li, J., Niu, S., Wang, C., Zhang, N., … Yang, Y. (2019). Effect of oxidized lipids stored under different temperatures on muscle protein oxidation in Sichuan-style sausages during ripening. *Meat Science, 147*, 144–154. https://doi.org/10.1016/j.meatsci.2018.09.008

Li, D., & Zhang, W. (2023). Biogenic amines and volatile N-nitrosamines in Chinese smoked-cured bacon (Larou) from industrial and artisanal origins. *Food Additives & Contaminants: Part B, 16*(2), 143–160. https://doi.org/10.1080/19393210.2023.2186489

Li, Y., Li, C., Li, H., Lin, X., Deng, S., & Zhou, G. (2016). Physicochemical and fatty acid characteristics of stewed pork as affected by cooking method and time. *International Journal of Food Science and Technology, 51*(2), 359–369. https://doi.org/10.1111/ijfs.12968

Maw, S. J., Fowler, V. R., Hamilton, M., & Petchey, A. M. (2003). Physical characteristics of pig fat and their relation to fatty acid composition. *Meat Science, 63*(2), 185–190. https://doi.org/10.1016/s0309-1740(02)00069-4

McLean, K. G., Hanson, D. J., Jervis, S. M., & Drake, M. A. (2017). Consumer perception of retail pork bacon attributes using adaptive choice-based conjoint analysis and maximum differential scaling. *Journal of Food Science, 82*(11), 2659–2668. https://doi.org/10.1111/1750-3841.13934

Okon, A., Szymanski, P., Zielinska, D., Szydlowska, A., Siekierko, U., Kolozyn-Krajewska, D., & Dolatowski, Z. J. (2021). The influence of acid whey on the lipid composition and oxidative stability of organic uncured fermented bacon after production and during chilling storage. *Antioxidants, 10*(11), 1711. https://doi.org/10.3390/antiox10111711

Paszkiewicz, W., Muszynski, S., Kwiecien, M., Zhyla, M., Swiatkiewicz, S., Arczewska-Wlosek, A., & Tomaszewska, E. (2020). Effect of soybean meal substitution by raw chickpea seeds on thermal properties and fatty acid composition of subcutaneous fat tissue of broiler chickens. *Animals, 10*(3), 533. https://doi.org/10.3390/ani10030533

Purslow, P. P. (2018). Contribution of collagen and connective tissue to cooked meat toughness; some paradigms reviewed. *Meat Science, 144*, 127–134. https://doi.org/10.1016/j.meatsci.2018.03.026

Sasaki, K., Mitsumoto, M., Nishioka, T., & Irie, M. (2006). Differential scanning calorimetry of porcine adipose tissues. *Meat Science, 72*(4), 789–792. https://doi.org/10.1016/j.meatsci.2005.09.020

Seman, D. L., Barron, W. N. G., & Matzinger, M. (2013). Evaluating the ability to measure pork fat quality for the production of commercial bacon. *Meat Science, 94*(2), 262–266. https://doi.org/10.1016/j.meatsci.2013.01.009

Tan, P., Wabike, E. E., Qin, G., Lou, B., Xu, D., Chen, R., & Wang, L. (2021). Effects of dietary n-3 long-chain polyunsaturated fatty acids (n-3 LC-PUFAs) on growth performance, body composition and subcutaneous adipose tissue transcriptome analysis of juvenile yellow drum (Nibea albiflora). *Aquaculture Nutrition, 27*(2), 556–567. https://doi.org/10.1111/anu.13206

Tu, T., Wu, W., Tang, X., Ge, Q., & Zhan, J. (2021). Screening out important substances for distinguishing Chinese indigenous pork and hybrid pork and identifying different pork muscles by analyzing the fatty acid and nucleotide contents. *Food Chemistry, 350*, Article 129219. https://doi.org/10.1016/j.foodchem.2021.129219

Walsh, M. M., Kerry, J. F., Buckley, D. J., Morrissey, P. A., Lynch, P. B., & Arendt, E. (1998). The effect of dietary supplementation with alpha-tocopheryl acetate on the stability of low nitrite cured pork products. *Food Research International, 31*(1), 59–63. https://doi.org/10.1016/s0963-9969(98)00061-1

Wang, Y., Wang, Z., Han, Q., Xie, Y., Zhou, H., Zhou, K., … Xu, B. (2022). Comprehensive insights into the evolution of microbiological and metabolic characteristics of the fat portion during the processing of traditional Chinese bacon. *Food Research International, 155*, Article 110987. https://doi.org/10.1016/j.foodres.2022.110987

Wijarnprecha, K., Fuhrmann, P., Gregson, C., Sillick, M., Sonwai, S., & Rousseau, D. (2022). Temperature-dependent properties of fat in adipose tissue from pork, beef and lamb. Part 2: Rheology and texture. *Food and Function, 13*(13), 7132–7143. https://doi.org/10.1039/d2fo00582d

Wijarnprecha, K., Gregson, C., Sillick, M., Fuhrmann, P., Sonwai, S., & Rousseau, D. (2022). Temperature-dependent properties of fat in adipose tissue from pork, beef and lamb. Part 1: Microstructural, thermal, and spectroscopic characterisation. *Food and Function, 13*(13), 7112–7122. https://doi.org/10.1039/d2fo00581f

Wu, W., Zhan, J., Tang, X., Li, T., & Duan, S. (2022). Characterization and identification of pork flavor compounds and their precursors in Chinese indigenous pig breeds by volatile profiling and multivariate analysis. *Food Chemistry, 385*, Article 132543. https://doi.org/10.1016/j.foodchem.2022.132543

Xie, J. C., Sun, B. G., & Wang, S. B. (2008). Aromatic constituents from chinese traditional smoke-cured bacon of mini-pig. *Food Science and Technology International, 14*(4), 329–340. https://doi.org/10.1177/1082013208098331

Xu, L., Cheng, J., Liu, X., & Zhu, M. (2019). Effect of microencapsulated process on stability of mulberry polyphenol and oxidation property of dried minced pork slices during heat processing and storage. *LWT-Food Science and Technology, 100*, 62–68. https://doi.org/10.1016/j.lwt.2018.10.025

Xu, Y., Xie, X., Zhang, W., Yan, H., Peng, Y., Jia, C., … Zhou, G. (2022). Effect of stewing time on fatty acid composition, textural properties and microstructure of porcine subcutaneous fat from various anatomical locations. *Journal of Food Composition and Analysis, 105*, Article 104240. https://doi.org/10.1016/j.jfca.2021.104240

Yang, Y., Zhang, X., Wang, Y., Pan, D., Sun, Y., & Cao, J. (2017). Study on the volatile compounds generated from lipid oxidation of Chinese bacon (unsmoked) during processing. *European Journal of Lipid Science and Technology, 119*(10), 1600512. https://doi.org/10.1002/ejlt.201600512

Zhang, J., Wang, T., Yang, C., Wu, R., Xi, L., & Ding, W. (2023). Integrated proteomics and metabolomics analysis revealed the mechanisms underlying the effect of irradiation on the fat quality of Chinese bacon. *Food Chemistry, 413*, Article 135385. https://doi.org/10.1016/j.foodchem.2023.135385

Zhang, M., Qiao, H., Zhang, W., Zhang, Z., Wen, P., & Zhu, Y. (2021). Tissue Type: A crucial factor influencing the fungal diversity and communities in Sichuan pork bacon. *Frontiers in Microbiology, 12*, Article 655500. https://doi.org/10.3389/fmicb.2021.655500

Zhu, H., Li, P., Wang, L., Huang, Q., & Xu, B. (2023). Flavor profile of “Dao Ban Xiang”(a traditional dry-cured meat product in Chinese Huizhou cuisine) at different processing stages in winter and summer. *Food Science & Nutrition, 11*(6), 2733–2750. https://doi.org/10.1002/fsn3.3225

Zhuang, X., Jiang, X., Han, M., Kang, Z. L., Zhao, L., Xu, X. L., & Zhou, G. H. (2016). Influence of sugarcane dietary fiber on water states and microstructure of myofibrillar protein gels. *Food Hydrocolloids, 57*, 253–261. https://doi.org/10.1016/j.foodhyd.2016.01.029